



Published in final edited form as:

*Nanotechnology*. 2017 February 17; 28(7): 075103. doi:10.1088/1361-6528/aa55e0.

## Facile Fabrication of Tissue-Engineered Constructs Using Nanopatterned Cell Sheets and Magnetic Levitation

Nisa Penland<sup>1,\*</sup>, Eunpyo Choi<sup>1,4,\*</sup>, Mikael Perla<sup>1</sup>, Jungyul Park<sup>4</sup>, and Deok-Ho Kim<sup>1,2,3,#</sup>

<sup>1</sup>Department of Bioengineering, University of Washington, Seattle, WA 98195

<sup>2</sup>Institute for Stem Cell and Regenerative Medicine, University of Washington, Seattle, WA 98109

<sup>3</sup>Center for Cardiovascular Biology, University of Washington, Seattle, WA 98109

<sup>4</sup>Department of Mechanical Engineering, Sogang University, Seoul, Korea

### Abstract

We report a simple and versatile method for *in vitro* fabrication of scaffold-free tissue-engineered constructs with predetermined cellular alignment, by combining magnetic cell levitation with thermoresponsive nanofabricated substratum (TNFS) based cell sheet engineering technique. The TNFS based nanotopography provides contact guidance cues for regulation of cellular alignment and enables cell sheet transfer, while magnetic nanoparticles facilitate the magnetic levitation of the cell sheet. The temperature-mediated change in surface wettability of the thermoresponsive poly(N-isopropylacrylamide), PNIPAM, substratum enables the spontaneous detachment of cell monolayers, which can then be easily manipulated through use of a ring or disk shaped magnet. Our developed platform could be readily applicable to production of tissue-engineered constructs containing complex physiological structures for the study of tissue structure-function relationships, drug screening, and regenerative medicine.

### Keywords

Thermoresponsive polymer; Magnetic levitation; Nanofabrication; Magnetic nanoparticle; Tissue engineering

### Introduction

One of the major challenges in tissue engineering is the production of functional 3D tissue models capable of recapitulating complex, physiologically-relevant structures<sup>1-3</sup>. We have previously developed a thermoresponsive nanofabricated substratum (TNFS) that enables the engineering of scaffold-free 3D tissues with improved function and structural organization<sup>4</sup>.

#Corresponding Author: Deok-Ho Kim, Ph.D., Assistant Professor, Department of Bioengineering, University of Washington, N410G William H Foegle Building, 3720 15<sup>th</sup> Ave NE Box 355061, Seattle, WA 98195 Phone: 1-206-616-1133 Fax: 1-206-685-3300 deokho@uw.edu.

\*These authors contributed equally to this work

### Competing Interests

D-H.K. is a co-founder of NanoSurface Biomedical Inc., and has uncompensated stock options in this company. E.C. is a scientific advisor of NanoSurface Biomedical Inc.

Functionalization of the nanofabricated substratum with temperature-sensitive poly(N-isopropylacrylamide), PNIPAM, provides several distinct advantages for tissue culture and engineering applications. Firstly, the ability to print nanoscale topographical cues, like nanoridges or grooves, allows for tunable control of the cellular microenvironment in order to direct and control global tissue organization. Previous studies have been shown that when cells are cultured on anisotropic nanopatterned substratum, the formation of highly organized anisotropic monolayers which closely resemble the *in vivo* structure of native human myocardial tissue are observed<sup>5-7</sup>. Moreover, both cellular action potential propagation and contractility are highly anisotropic and consistent with the underlying nanotopographic cues. This suggests that the anisotropic nanopatterned substratum provide powerful guidance cues regulating cellular alignment and function *in vitro*. Lastly, methods utilizing thermoresponsive polymers have previously been used to fabricate cell-dense 3D tissue structures without scaffold-based tissue engineering techniques<sup>4, 8-10</sup>. The change in hydrophobicity of PNIPAM from hydrophobic, at physiological temperatures (37°C), to hydrophilic, at ambient room temperatures (22°C), allows for the selective detachment of either individual cells or cellular monolayers without the use of extracellular matrix (ECM)-digesting enzymes or calcium chelators (i.e. Trypsin-EDTA). However, despite the advantages of the TNFS platform, controlling and manipulating the released cell sheet is difficult because the competition between bending and stretching forces within thin cell monolayers cause them to roll inward spontaneously, which in turn leads to the loss of their anisotropic morphology. We previously developed a gel casting method to reduce this technical difficulty<sup>4</sup>, but this protocol is limited to 2D cell sheet transfer and low throughput applications. The capacity for TNFS technology to extend its benefits to other tissue culture platforms is therefore predicated on the development of novel manipulation methods with greater flexibility, control, and utility in 3D culture systems.

In this paper, we developed a simple and versatile method for performing magnetic nanoparticle-mediated cell sheet transfer that enables the long-term maintenance of structural organization. In addition, we established a scaffold-free 3D tissue culture method for creating cell spheroids with predetermined cellular alignment using magnetic nanoparticles in combination with the TNFS platform. Nanoparticles have been utilized for many bioengineering-based applications, such as drug delivery<sup>11, 12</sup>, bio-imaging<sup>13, 14</sup>, artificial cell culture platform<sup>15, 16</sup>, anti-fouling<sup>17, 18</sup>, and antibacterial coatings<sup>19, 20</sup>. Previously, magnetic nanoparticles have been used to create three dimensional (3D) tissue culture platforms via magnetic levitation<sup>21-24</sup>. Cellular binding of magnetic nanoparticles allows for external manipulation of cellular function using an external magnetic field<sup>25-27</sup>. Magnetic levitation provides a physiologically relevant 3D culture environment that could promote the formation of complex structures and more mature phenotypes currently limited by conventional 2D culture systems.

To utilize this magnetic levitation in our proposed system, the magnetic nanoparticle embedded cells were cultured on TNFS. Aligned cell monolayers that closely mimic the architectures of native cellular environments were then created by nanotopographic cues. Lastly, these cell monolayers were detached spontaneously, as intact cell sheets, and manipulated through the application of ring or disk shaped magnets to facilitate cell sheet transfer and the formation of 3D scaffold-free spheroid-shaped tissues. We believe that the

proposed platform could be used to study cellular microenvironments and the organization and composition of ECM within 3D tissues models.

## Materials and Methods

### Fabrication of Thermo-responsive Nanofabricated Substratum (TNFS)

Figure 1 shows schematic diagrams that describe the procedures for fabricating a poly(urethane acrylate)-poly(glycidyl methacrylate) nanopatterned substratum, as reported previously<sup>4</sup>. Briefly, using capillary force lithography<sup>28</sup>, a UV-curable poly(urethane acrylate) (PUA, Minutatek, Korea) mold was fabricated using a silicone master. This mold was used as the template for reproducing nanotopography on treated glass using a 1% weight/volume GMA (Sigma-Aldrich)/PUA (Norland Optical Adhesive) solution. Prior to nanopattern fabrication, glass coverslips were brush coated with an adhesion promoter and air-dried (Glass Primer, Minuta Tech, Korea) to improve the attachment of the GMA/PUA polymer to the glass surface. 20  $\mu$ L of GMA/PUA solution was applied to the coverslip and pressed with the PUA template consisting of 800 nm wide and 800 nm deep parallel grooves and ridges. The GMA/PUA solution was drawn up into the nanogrooves of the PUA mold via capillary force, and then the mold/GMA-PUA/glass sandwich was cured under 365 nm UV light to initiate photo polymerization for 5 minutes. After initial polymerization, the PUA mold was peeled away from the new nanopatterned substratum using forceps and the substratum were UV-cured overnight to finalize polymerization.

The epoxy groups present within GMA of the GMA/PUA substratum react freely with the amine groups presented by amine-terminated poly(N-isopropylacrylamide) ( $\alpha$ -PNIPAM) through an addition reaction to form a hydroxyl group and a secondary amine (Figure 1). Powdered  $\alpha$ -PNIPAM ( $M_n = 2500$ , Sigma-Aldrich) was dissolved in deionized (DI) water at room temperature at a concentration of 1 g/30 mL. In order to thermo-responsively functionalize the nanofabricated GMA/PUA substratum, the PNIPAM solution was reacted with the GMA/PUA substratum on a table-top rocker at room temperature for 24 hours at 55 rpm. The TNFS were then washed three times with DI water and sterilized with 294 nm UV light for one or more hours prior to use.

### Cell Culture and Seeding on the TNFS

C2C12 mouse myoblasts were cultured in Dulbecco's minimal essential medium (DMEM, Gibco) supplemented with 20% fetal bovine serum (FBS, Sigma), 1% penicillin-streptomycin (Sigma), and 1% amphotericin-B (Sigma) in an incubator at 37 °C, 5% CO<sub>2</sub>. Cells were split at 80% confluency to prevent spontaneous differentiation. To seed cells onto the TNFS, cells were split and seeded at either a low density (75,000 cells/plate = 48,700 cells/cm<sup>2</sup>) for cell spheroid levitation or a high density (150,000 cells/plate = 97,500 cells/cm<sup>2</sup>) for cell sheet transfer. In order to ensure cells were only seeded onto the PNIPAM functionalized surface within the 35 mm dishes, cells were re-suspended in a small volume of 120  $\mu$ L of culture medium and plated into the recessed well that is created by the nanopatterned coverslip once attached to the underside of the 35 mm dish in order to seal the hole at its bottom. The plates were lightly shaken to evenly distribute the cells across the surface of the TNFS, and incubated at 37°C for 2 hours to allow cell attachment. Warmed

medium was then added to each dish for further culturing. Cells were cultured for 24 to 48 hours at 37 °C to allow sufficient cell attachment before addition of the nanoparticle assembly. Cells cultures were imaged using a bright-field microscope (Nikon TS100).

### **Attachment of Nanoparticles for Cell Sheet Transfer**

For the plates seeded at a higher density (150,000 cells/plate = 97,500 cells/cm<sup>2</sup>), medium was removed 48 hours after plating and 120 µL of culture medium with 1 µL/10,000 cells of Nanoshuttle™-PL (Nano3D Biosciences, Inc., USA) was added to the cell sheet. The Nanoshuttle product consists of a composite nanoparticle (~50 nm) consisting of gold, iron oxide, and poly-L-lysine (PLL) that can attach to the plasma membrane electrostatically (50 pg/cell). The cell sheets were incubated for one hour at 37°C before the addition of 2 mL warmed medium. Finally, they were incubated overnight with the nanoparticle assembly and cellular uptake of the nanoparticles was confirmed using bright field microscopy.

### **Attachment of Nanoparticles for Spheroid Levitation**

For the plates seeded at a lower density (48,700 cells/cm<sup>2</sup>), medium was removed 24 hours after plating and 120 µL of culture medium with 1 µL/10,000 cells of Nanoshuttle™-PL was added and allowed to incubate for one hour<sup>21</sup>. Following the initial incubation period, 2 mL cell culture medium was added to each sample, taking care to minimize any disturbance of the nanoparticle solution. Cell cultures were incubated overnight in the solution of medium and nanoparticles. Uptake of the nanoparticles was again confirmed using bright field microscopy.

### **Immunofluorescence Cryosectioning and Staining**

Cell spheroids were washed twice with PBS for 5 minutes with centrifugation at 1000 rpms for 1 minute in between each wash. 100 µL of 4% paraformaldehyde was then added to fix the cells at room temperature for 15 minutes. After fixation, cells were washed 3 times with PBS with centrifugation. Cell spheroids were then placed into cryomolds and filled with optimal cutting temperature (OCT) compound so that the entire spheroid was immersed. The cryomold was then dipped, but not submerged, into liquid nitrogen to flash freeze the sample. The frozen tissue block was then transferred into a cryotome cryostat at -20°C. The spheroids were sectioned into 5 µm slices and mounted onto glass microscope slides.

On the microscope slides, cells were permeabilized and blocked with a 0.1% Triton-X100/5% BSA-PBS solution for one hour at room temperature. Phalloidin (1:100) and fibronectin (1:200) primary antibody were added to a 1% BSA-PBS solution, then the 100 µL composite solution was added to the cells and was incubated over night at 4°C. The cells were then washed in 1 mL of PBS 3 times for 5 minutes before being mounted on microscope slides using a Vectashield mounting medium. Nuclear counterstaining was achieved by incorporation of DAPI into the mounting medium. Samples were sealed with nail polish and stored at 4°C until ready for analysis. Immunofluorescent imaging was performed on a confocal microscope (Model 36 LSM 510 Meta, Zeiss Confocal Microscope) and using the associated software.

## Magnetic Levitation

Disk shaped neodymium magnets with a diameter of 25.4 mm and a thickness of 1.6 mm (N52 strength, K&J Magnetics, Inc., USA) and ring shaped neodymium magnets (outer diameter: 32 mm, hole diameter, 5.5 mm, and thickness: 8 mm, N42 strength, Gaussboys Super Magnets, USA) were used throughout this study. The Teflon-based magnet housing for the cell transfer system was designed using 3D CAD software (SolidWorks, USA) and fabricated using a 3D printer (Makerbot, USA) with the following dimensions: inner diameter = 27 mm, outer diameter = 32 mm, height = 20 mm, and “Vent” diameters = 3 mm.

## Results and Discussion

We fabricated TNFS containing 1% GMA by weight (Figure 2A) based on previous work that showed that C2C12 mouse myoblast cells exhibited increased attachment and improved monolayer formation with decreasing GMA percentages, suggesting that high-density grafted PNIPAM inhibited cell adhesion<sup>4</sup>. Specifically, the 1% GMA TNFS produced the most confluent monolayers of all GMA concentrations studied. Similarly, nanotopographical cues consisting of parallel ridges and grooves with dimensions 800 nm wide and 800 nm deep were fabricated since previous studies indicated these dimensions were optimal for promoting cellular development<sup>7</sup>. Scanning electron microscopy (SEM) confirmed nanopattern fidelity in our engineered constructs (Figure 2A inset).

To demonstrate the control over 3D tissue architecture provided by TNFS and magnetic levitation, C2C12 mouse myoblasts were used for all experiments. Figure 2B and C show phase contrast images of C2C12 myoblasts cultured on flat control substratum and TNFS, respectively. Cells attached to the flat control substratum and TNFS within 2 hours of seeding and spread to form a confluent monolayer within 24 hours. Cells cultured on TNFS showed rapid formation and alignment in parallel with the direction of the nanopatterns within 2 hours of seeding, indicating cellular sensitivity to nanoscale topography. Figure 2D shows bright field microscopic images indicating the uptake of nanoparticles by individual cells within the cell sheet cultured on TNFS after incubation with Nanoshuttle (brown particles). The black arrow denotes the direction of cell alignment within the cell sheet and TNFS. Cell sheets could be maintained in culture with the nanoparticle assembly for several days without any observable adverse effects on cell morphology, growth, or structural anisotropy.

To conduct thermoresponsive detachment of cell monolayers from TNFS, the nanoparticle embedded C2C12 monolayer maintained on 1% GMA TNFS was transferred from a 37°C culture incubator to room temperature (22 °C). In addition, room temperature DPBS was applied to the cells to induce the temperature-mediated change in substratum configuration. Within 10 min, the medium began to penetrate the edges of the C2C12 monolayer and buckling, *i.e.*, delamination and folding was observed, as shown in Figure 2E: because of a competition between bending and stretching within the thin cell monolayer, the sheet rolled inward on itself (yellow arrow) perpendicular to the alignment angle (black arrow). Subsequently, the cell sheet quickly began to lose its anisotropic morphology and became a cell-dense mass due to the spontaneous curling and tube formation properties of the detached cell monolayer.

In order to avoid the loss of structural organization and anisotropic morphology while transferring or manipulating the detached cell sheets, we introduced a cell sheet transfer method using magnetic levitation. Schematic illustration of the cell sheet transfer process using a disk shaped magnet is shown in Figure 3A. A Teflon-coated magnetic transfer device, consisting of a custom 3D-printed housing with a N52 strength disk magnet with a diameter of 25.4 mm and a thickness of 1.6 mm (K&J Magnetics, Inc., USA) was placed directly on top of the cultured cell sheet. The cell sheet was then detached from the TNFS via incubation in DPBS at room temperature (22 °C). Once the cell sheet had detached, the remaining liquid was aspirated from the culture dish and the magnetic transfer device was lifted from the dish with the cell sheet remaining fixed to the bottom of the transfer device. Figure 3B shows a detached nanoparticle embedded C2C12 cell sheet from TNFS affixed to the bottom of the magnetic transfer device without losing structural organization. The red arrow denotes the direction of cell alignment within the cell sheet. Once detached, the housing and levitated cell sheet was then placed onto a glass surface treated with fetal bovine serum (FBS) to aid cell attachment. The magnet within the housing was then removed and placed underneath the culture dish to encourage attachment. The entire construct was incubated at 37 °C for three hours to allow for cell sheet attachment to the glass. The transfer device was lifted off leaving the cell sheet attached to the new culture surface and warm medium was gently added. As shown in Figure 3C, we demonstrated that magnetic levitation can enable the successful transfer of a nanoparticle embedded C2C12 cell sheet to a new glass substratum.

In addition to transferring intact sheets, we investigated the potential to create scaffold-free 3D tissue culture via production of cell spheroids with predetermined cellular alignment through use of magnetic levitation in combination with the TNFS platform. First, a sphere-shaped scaffold-free tissue culture was created, as shown in Figure 4. A ring shaped neodymium magnet (outer diameter: 32 mm, hole diameter, 5.5 mm, and thickness: 8 mm, Gaussboys Super Magnets, USA) was used for this application because the ring's hole made it possible to observe the cells through the inverted microscope. In addition, this magnet was able to gather the cells in the center of the well to form a spheroidal cell tissue. Magnetic flux simulations of a planner magnet<sup>29</sup> using commercial finite element software COMSOL Multiphysics® demonstrate that when the distance between the ring shaped magnet and working plane (cell sheet) is less than 6 mm, the magnetic field on the working plane possesses central minimum (Figure 4B). This leads to a ring-shaped cell pattern at the onset of levitation produced by the upward force pulling cells towards the field maximum<sup>21</sup>. However, when the magnet is placed far enough from the work plane (greater than 6 mm above), the central maximum of the magnetic field was produced (Figure 4B), resulting in the ability to form sphere shaped tissues. In this experiment, the distance between the ring magnet and the cell sheet was 12 mm which should result in the formation of 3D cell spheroids.

Subsequent experimental results showed good agreement with the simulation result. To create spheroid cell structures, culture medium was aspirated and replaced with room temperature (22 °C) DPBS to induce a temperature change. The ring shaped magnet was then immediately placed 12 mm above the cell-sheet. 10 minutes after the thermal shift, the cells on TNFS began to spontaneously detach, magnetically levitate, and gathered at the

center of the ring shaped magnet (Figure 4C). The cell mass formed within 48 hours of levitation and took on spherical shape with 72 hours. The spheroids maintained their shape over 5 days in a levitated state. Figure 4D shows confocal images of the C2C12 cell sphere after 5 days in levitation. Expression of F-actin filaments were observed throughout the entire structure as well as areas of locally aligned cells (white arrow denotes direction of cell alignment within the cell sheet). Upon magnetic levitation of nanopatterned cell sheets into spheroid form, cellular alignment becomes less pronounced than nanopatterned cell sheets maintained on TNFS as shown in Figure 2D. Within the levitated spheroid, the surface topographical cues provided by the TNFS are no longer present, and cells respond to the changing matrix guidance cues provided by the surrounding 3D extracellular matrix (ECM).

With such results, these methods could be readily expanded to a number of other cell types to create more structurally ordered tissues compared to conventional cell culture methods. Our recent study showed that anisotropic nanotopography was sufficient to distinguish structural differences between normal human induced pluripotent stem cell derived cardiomyocytes (hiPSC-CMs) and Duchenne muscular dystrophy (DMD) hiPSC-CMs, as these differences were masked on conventional flat substratum<sup>30</sup>. With further investigation, we envision significant improvements in the engineering of complex and physiological tissues such as multi-layered, uniformly-aligned, 3D tissues for drug screening and disease modeling applications.

## Conclusion

In this study, we combined TNFS-based cell culture platforms with magnet levitation techniques for both the transfer of intact cell sheets and the formation of scaffold-free spheroids. Cell sheets could be quickly and spontaneously released from the TNFS by a temperature change, eliminating the need for cell-disassociating agents such as Trypsin-EDTA. Our TNFS, in combination with magnetic nanoparticle technology, has allowed us to create 3D tissues with complex cellular architectures produced by the natural secretion of ECM proteins. These methods could be used to study cellular microenvironments, cell migration, and organization of ECM proteins within 3D tissues models. Future studies will assess the long-term structural maintenance of the ECM in levitated cultures and the effects of levitation on the differentiation and maturation of other cell types.

## Acknowledgments

This work was supported by the National Institutes of Health under award numbers (R21AR064395 to D-H.K. and R01NS094388) and National Research Foundation of Korea (NRF) grant funded by the Korean government (MSIP) (NRF-2013R1A1A2073271 to E.C. and J.P.). The authors thank Dr. Alex Jiao for his technical assistance in TNFS fabrication and Dr. Alec Smith for his assistance in editing this manuscript.

## References

1. Antoni D, Burckel H, Josset E, et al. Three-dimensional cell culture: a breakthrough in vivo. *International Journal of Molecular Sciences*. 2015; 16:5517–5527. [PubMed: 25768338]
2. Gauvin R, Khademhosseini A. Microscale technologies and modular approaches for tissue engineering: moving toward the fabrication of complex functional structures. *ACS Nano*. 2011; 5:4258–4264. [PubMed: 21627163]

3. Griffith LG, Swartz MA. Capturing complex 3D tissue physiology in vitro. *Nature Reviews Molecular Cell Biology*. 2006; 7:211–224. [PubMed: 16496023]
4. Jiao A, Trosper NE, Yang HS, et al. Thermoresponsive Nanofabricated Substratum for the Engineering of Three-Dimensional Tissues with Layer-by-Layer Architectural Control. *ACS Nano*. 2014; 8:4430–4439. [PubMed: 24628277]
5. Kim DH, Kshitiz, Smith RR, et al. Nanopatterned cardiac cell patches promote stem cell niche formation and myocardial regeneration. *Integrative Biology*. 2012; 4:1019–1033. [PubMed: 22890784]
6. Kshitiz, Park J, Kim P, et al. Control of stem cell fate and function by engineering physical microenvironments. *Integrative Biology : Quantitative Biosciences from Nano to Macro*. 2012; 4:1008–1018. [PubMed: 23077731]
7. Carson D, Hnilova M, Yang X, et al. Nanotopography-Induced Structural Anisotropy and Sarcomere Development in Human Cardiomyocytes Derived from Induced Pluripotent Stem Cells. *ACS Applied Materials & Interfaces*. 2016; 8:21923–21932. [PubMed: 26866596]
8. Haraguchi Y, Shimizu T, Sasagawa T, et al. Fabrication of functional three-dimensional tissues by stacking cell sheets in vitro. *Nature Protocols*. 2012; 7:850–858. [PubMed: 22481530]
9. Takahashi H, Shimizu T, Nakayama M, et al. The use of anisotropic cell sheets to control orientation during the self-organization of 3D muscle tissue. *Biomaterials*. 2013; 34:7372–7380. [PubMed: 23849343]
10. Williams C, Xie AW, Yamato M, et al. Stacking of aligned cell sheets for layer-by-layer control of complex tissue structure. *Biomaterials*. 2011; 32:5625–5632. [PubMed: 21601276]
11. Verma SK, Arora I, Javed K, et al. Enhancement in the Neuroprotective Power of Riluzole Against Cerebral Ischemia Using a Brain Targeted Drug Delivery Vehicle. *ACS Applied Materials & Interfaces*. 2016; 8:19716–19723. [PubMed: 27378322]
12. Han J, Zhen J, Du Nguyen V, et al. Hybrid-Actuating Macrophage-Based Microrobots for Active Cancer Therapy. *Scientific Reports*. 2016; 6:28717. [PubMed: 27346486]
13. Sharma P, Brown S, Walter G, et al. Nanoparticles for bioimaging. *Advances in Colloid and Interface Science*. 2006; 123–126:471–485.
14. Gonzalez-Bejar M, Frances-Soriano L, Perez-Prieto J. Upconversion Nanoparticles for Bioimaging and Regenerative Medicine. *Frontiers in Bioengineering and Biotechnology*. 2016; 4:47. [PubMed: 27379231]
15. Fiorini F, Prasetyanto EA, Taraballi F, et al. Nanocomposite Hydrogels as Platform for Cells Growth, Proliferation, and Chemotaxis. *Small*. 2016; 12:4881–4893. [PubMed: 27364463]
16. Choi E, Chang HK, Lim CY, et al. Concentration gradient generation of multiple chemicals using spatially controlled self-assembly of particles in microchannels. *Lab on a Chip*. 2012; 12:3968–3975. [PubMed: 22907568]
17. Boyer C, Priyanto P, Davis TP, et al. Anti-fouling magnetic nanoparticles for siRNA delivery. *Journal of Materials Chemistry*. 2010; 20:255–265.
18. Das SK, Khan MM, Parandhaman T, et al. Nano-silica fabricated with silver nanoparticles: antifouling adsorbent for efficient dye removal, effective water disinfection and biofouling control. *Nanoscale*. 2013; 5:5549–5560. [PubMed: 23680871]
19. Xie X, Wang L, Xing D, et al. Protein-repellent and antibacterial functions of a calcium phosphate rechargeable nanocomposite. *Journal of Dentistry*. 2016; 52:15–22. [PubMed: 27327110]
20. Richter AP, Brown JS, Bharti B, et al. An environmentally benign antimicrobial nanoparticle based on a silver-infused lignin core. *Nature Nanotechnology*. 2015; 10:817–823.
21. Souza GR, Molina JR, Raphael RM, et al. Three-dimensional tissue culture based on magnetic cell levitation. *Nature Nanotechnology*. 2010; 5:291–296.
22. Molina JR, Hayashi Y, Stephens C, et al. Invasive glioblastoma cells acquire stemness and increased Akt activation. *Neoplasia*. 2010; 12:453–463. [PubMed: 20563248]
23. Daquinag AC, Souza GR, Kolonin MG. Adipose tissue engineering in three-dimensional levitation tissue culture system based on magnetic nanoparticles. *Tissue Engineering Part C, Methods*. 2013; 19:336–344. [PubMed: 23017116]



24. Jeong YG, Lee JS, Shim JK, et al. A scaffold-free surface culture of B16F10 murine melanoma cells based on magnetic levitation. *Cytotechnology*. 2016; doi: 10.1007/s10616-10016-10026-10617.
25. Ito A, Ino K, Kobayashi T, et al. The effect of RGD peptide-conjugated magnetite cationic liposomes on cell growth and cell sheet harvesting. *Biomaterials*. 2005; 26:6185–6193. [PubMed: 15899515]
26. Dobson J. Remote control of cellular behaviour with magnetic nanoparticles. *Nature Nanotechnology*. 2008; 3:139–143.
27. Durmus NG, Tekin HC, Guven S, et al. Magnetic levitation of single cells. *Proceedings of the National Academy of Sciences of the United States of America*. 2015; 112:E3661–3668. [PubMed: 26124131]
28. Macadangdang J, Lee HJ, Carson D, et al. Capillary force lithography for cardiac tissue engineering. *Journal of Visualized Experiments : JoVE*. 2014:e50039.
29. Shute HA, Mallinson JC, Wilton DT, et al. One-sided fluxes in planar, cylindrical, and spherical magnetized structures. *IEEE Transactions on Magnetics*. 2000; 36:440–451.
30. Macadangdang J, Guan X, Smith AST, et al. Nanopatterned Human iPSC-Based Model of a Dystrophin-Null Cardiomyopathic Phenotype. *Cellular and Molecular Bioengineering*. 2015; 8:320–332. [PubMed: 26366230]

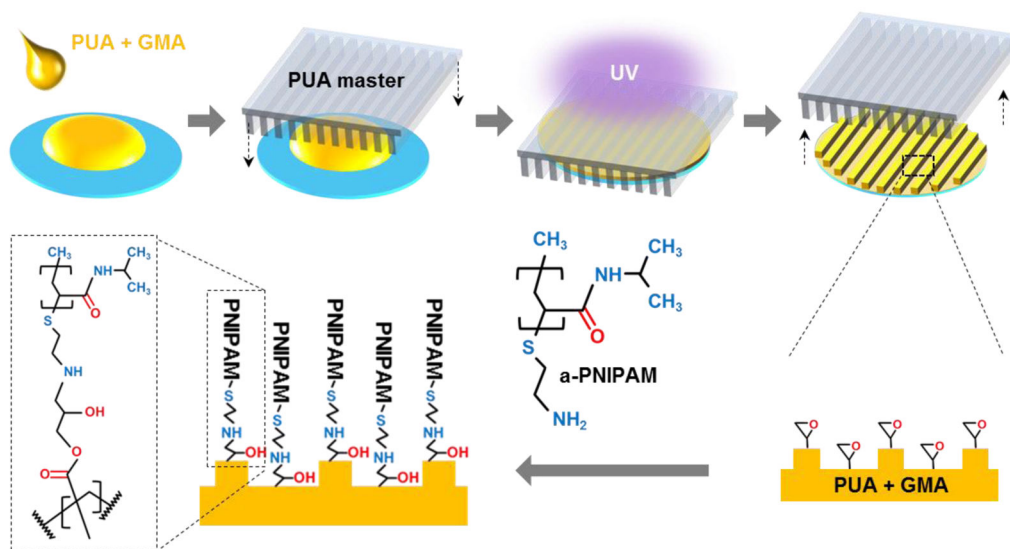


**Figure 1.** Schematic illustrations of the fabrication process used to create thermoresponsive nanofabricated substratum (TNFS) using capillary force lithography, and the subsequent functionalization of the substratum with amine-terminated PNIPAM.

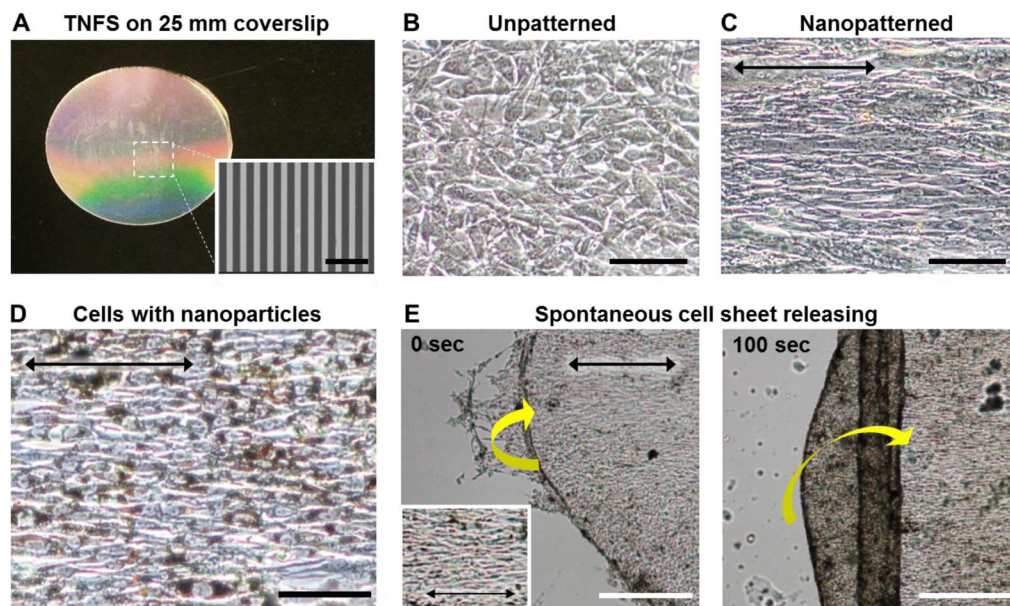


**Figure 2. Characterization of thermoresponsive nanofabricated substratum (TNFS) and C2C12 cell responses on TNFS. (A)** Photograph of fabricated TNFS and SEM image of nanopatterns (inset) on the TNFS. Bright field images of C2C12 myoblasts maintained on unpatterned (B) and nanopatterned (C) TNFS. (D) Bright field microscopic image of nanoparticle embedded C2C12 cells maintained on nanopatterned TNFS for 4 days. The black arrows denote direction of cell alignment within the cell sheet. (E) Time sequence bright field microscopic images of the cell-rolling phenomenon. Sheet was rolling perpendicular to cell alignment denoted by black arrow. Inset provides close-up detail of cell. Scale bars: 5  $\mu\text{m}$  in (A) and 100  $\mu\text{m}$  in (B), (C), (D), and 200  $\mu\text{m}$  in (E).

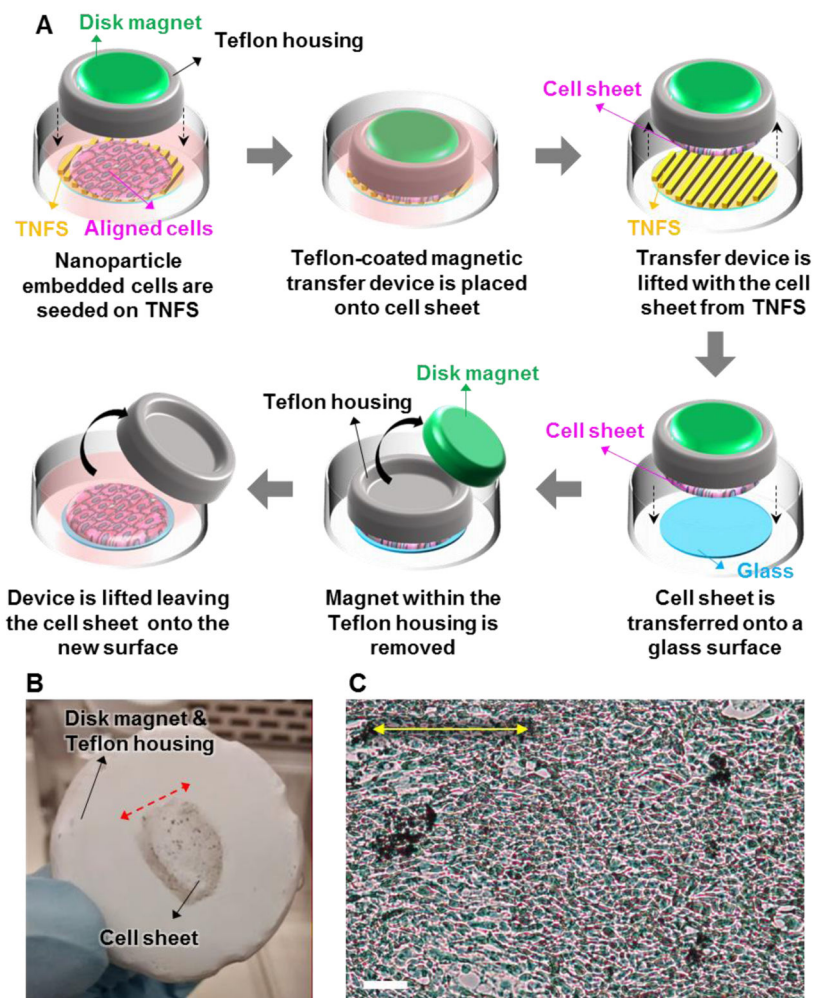


**Figure 3. Cell sheet transfer using thermoresponsive nanofabricated substratum (TNFS) based cell sheet engineering technique and magnetic cell levitation. (A)** Schematic illustrations of the cell sheet transfer process using a disk shaped magnet. A Teflon-coated magnetic transfer device was directly placed on top of the aligned cell sheet. The cell sheet was then detached from the TNFS via a reduction in culture temperature. The magnetic transfer device was lifted from the dish with the cell sheet remaining fixed to the bottom of the transfer device. The cell sheet and housing were then placed onto a glass surface. The magnet within the housing was then removed and placed underneath the culture dish to encourage attachment. Lastly, the transfer device was lifted off, leaving the cell sheet attached to the new culture surface. **(B)** Picture of the cell sheet transfer device and C2C12 cell sheet remaining fixed to the bottom of the transfer device. **(C)** C2C12 cell sheet 1 hour after transfer to glass. The yellow arrow denotes the direction of alignment within the cell sheet. Scale bar: 100  $\mu$ m in (C).

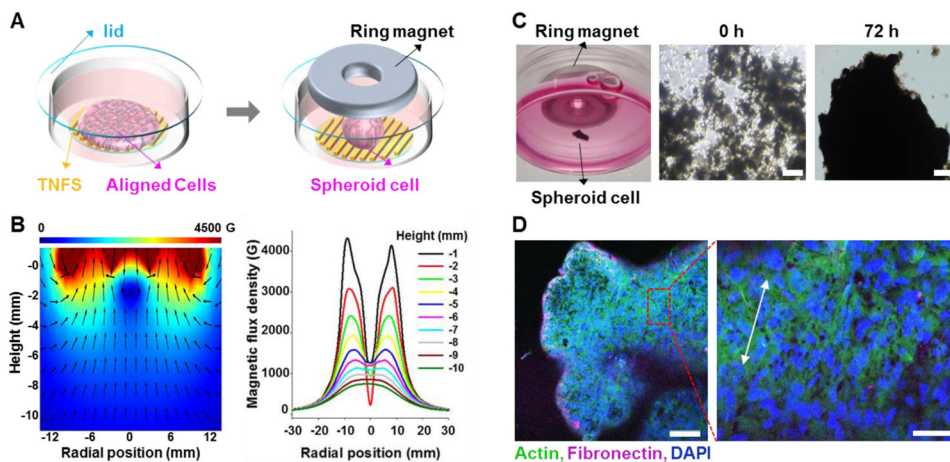


**Figure 4. Scaffold-free tissue construction with 3D sphere architecture.** (A) Schematic illustrations of sphere-shaped scaffold-free tissue culturing using ring shaped magnets. Following a temperature change in the cultured cells, the ring shaped magnet was placed above the cell-sheet. 10 minutes after temperature reduction, the cells on TNFS began to detach and magnetically levitated before gathering at the center of the ring shaped magnet. (B) Simulation results by COMSOL Multiphysics®. When the distance between the ring shaped magnet and the work plane (cell sheet) was less than 6 mm, the magnetic field on the work plane had a central minimum and was maximized surround the ring hole. However, when the magnet was far enough from the work plane (greater than 6 mm above), the central maximum of the magnetic field was produced promoting the formation of sphere shaped tissues. (C) Picture of C2C12 cells in levitation with ring-shaped magnet for 0 and 72 hours. (D) Confocal image of C2C12 sphere after 5 days in levitation. White arrow denotes direction of cell alignment within the cell sheet. Scale bars: 200  $\mu\text{m}$  in (C) and 100  $\mu\text{m}$  (left) and 50  $\mu\text{m}$  (right) in (D).